ELSEVIER

Polymer 41 (2000) 2095–2104

polymer

Phonon dispersion and heat capacity in cross-β form of poly(*O*-acetyl, L-serine)

N.K. Misra, D. Kapoor, P. Tandon, V.D. Gupta*

Department of Physics, University of Lucknow, Lucknow 226 007, India

Received 15 March 1999; received in revised form 25 May 1999; accepted 4 June 1999

Abstract

Poly(*O*-acetyl, L-serine), which is a precursor of poly(L-serine) in synthesic sequence, is found to exist in cross-β conformation. Normal mode analyses including phonon dispersion have been performed, to understand completely the FTIR spectra of this polypeptide, using Wilson's GF matrix method and Urey–Bradley force field. The characteristic features of dispersion curves like repulsion, exchange of character and bunching have been observed and discussed. In addition to the above the heat capacity is calculated as a function of temperature via density-of-states derived from dispersion curves.

Keywords: Poly(*O*-acetyl, L-serine); Normal mode analysis; Phonon dispersion

1. Introduction

In a recent publication in this journal the authors have reported a study of the dispersion of normal modes in 1,4 trans poly(1,3-pentadiene) [1]. In continuation of this work we are reporting, in the present communication, a study of phonon dispersion and heat capacity of poly(*O*-acetyl, L-serine) (PALS), which is a polypeptide. The conformational studies on PALS, which is a precursor of poly(L-serine) (PLS), in synthesic sequence, have been extensively carried out by Fasman and Blout [2]. On the basis of rotatory dispersion of PALS they proposed a parallel-β structure to this polymer. Later on Imahori and Yahara [3], in their study of optical properties and conformations of PALS and PLS on the basis of infrared spectroscopy, have shown that depending upon the mode of preparation for solid films of PALS two conformations are observed. The one obtained by directional rubbing of very viscous solution of PALS in trifluoro acetic acid was found to have a cross-β structure while the other obtained by strong rubbing in one direction was shown to be in a parallel-β structure. Cross-β conformation is essentially an antiparallel-β form but involves only a single chain which folds back on itself to form intra-chain hydrogen bonds [4]. This type of structure is found to be present in fibrous proteins like keratin [5], epidermin [5], myosin [5] and silk [6], in globular proteins and in several linear polypeptides [7] and cyclic polypeptides including peptide hormones [8] and antibodies [9]. On the basis of X-ray diffraction and birefringence measurements, Imahori et al. [3] showed that PALS exists in a cross-β conformation rather than a parallel-β structure. They have also performed optical rotatory dispersion measurements on PALS in dichloroacetic acid (25%)–chloroform (75%) solution and concluded that in solution also PALS exists in cross-β conformation with a small amount of random coil conformation. X-ray diffraction studies suggest that the unit cell of PALS in cross-β conformation is orthorhombic with $a = 9.6$, $b = 6.48$ and $c = 9.71$ Å. The characterization of PALS conformation may throw light on the study of the conformations of γ-globulin and epidermin which have a high content of serine compared with normal proteins.

Vibrational spectroscopy plays an important role in polypeptide characterization, determining crystallinity, conformation, intra- and inter-molecular hydrogen bonding, fold structure of polymers, composition and sequence distribution in copolymers. Recently much work has been reported on phonon dispersion on a variety of polymeric systems [10–14]. The present authors have demonstrated its potential in fuller interpretation of complex IR and Raman spectra through dispersion curves which are also essential for understanding the behavior of polymers at the microscopic level. Dispersion curves also provide information on the interactions of a given mode along the chain. Further, the frequency distribution function obtained from

* Corresponding author. Fax: +91-522-223405.

0032-3861/00/$ - see front matter
PII: S0032-3861(99)00395-X

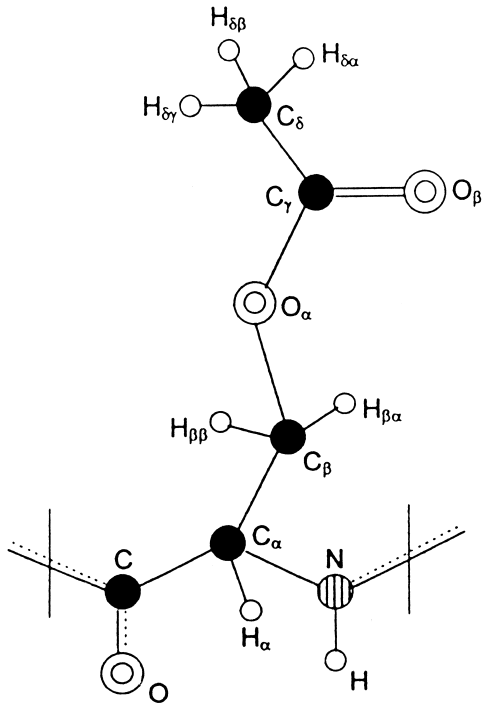

Fig. 1. Chemical repeat unit of PALS.

the dispersion curves may be used to calculate the elastic and thermodynamical properties such as heat capacity, entropy and enthalpy changes of polymers. In this way dispersion curves can be used to correlate the microscopic behavior with the macroscopic properties.

To the best of our knowledge no work on phonon dispersion of PALS has been reported so far. In the present study normal modes and their dispersion within the first Brillouin zone have been calculated for PALS. Calculated frequencies compare well with the peaks observed in the recorded FTIR spectra and the agreement between the two is found to be reasonably good. Frequency distribution function derived from dispersion curves is used to calculate the heat capacity in the temperature range 50–500 K.

2. Experiment and theory

The sample of PALS was purchased from Sigma Chemicals, USA (P 7142, Lot no. 32F50671, DP(vis) 91, MW(vis) 11,700). The Fourier transform infrared (FTIR) spectra were recorded on a Perkin Elmer 1800 spectrometer. The sample was prepared by mixing the sample in CsI and pressing in the form of a pellet. Before recording the spectra the equipment was purged with dry nitrogen.

2.1. Calculation of normal mode frequencies

The calculation of normal mode frequencies was carried out according to Wilson's GF matrix method [15,16] as modified by Higgs [17] for an infinite polymeric chain. In brief, the vibrational secular equation, which gives the normal mode frequencies, has the form

$$|G(\delta)F(\delta) - \lambda(\delta)I| = 0 \qquad 0 \leq \delta \leq \pi \tag{1}$$

where G is the inverse kinetic energy matrix, F the potential energy matrix and δ is the vibrational phase difference between the corresponding modes of adjacent residue units.

The vibrational frequencies $\nu_i(\delta)$ (in cm^{-1}) are related to the eigenvalues $\lambda_i(\delta)$ by the following relation:

$$\lambda_i(\delta) = 4\pi^2 c^2 \nu_i^2(\delta) \tag{2}$$

A plot of $\nu_i(\delta)$ versus δ gives the dispersion curve for the ith mode.

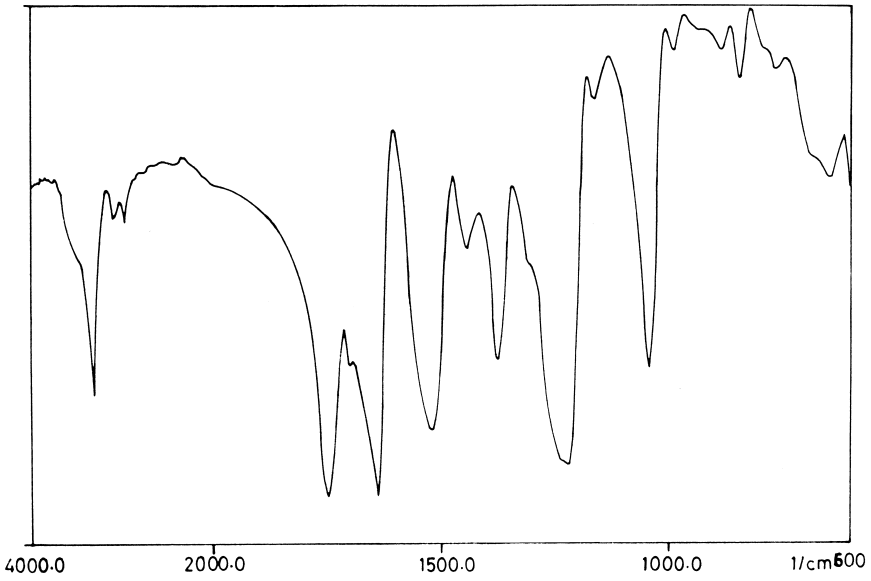

Fig. 2. FTIR spectra of PALS (4000–600 cm^{-1}).

Table 1
Internal coordinates and force constants (md/Å) (ν, ϕ, ω, τ denote stretch, anglebend, wag and torsion, respectively; stretching force-constants between the nonbonded atoms in each angular triplet (gem configuration) are given in parentheses)

Internal coordinate	Force constant	Internal coordinate	Force constant
ν[C–Cα]	2.34	ϕ[C–Cα–Hα]	0.36 (0.20)
ν[Cα–H]	4.167	ϕ[C–Cα–Cβ]	0.43 (0.20)
ν[Cα–N]	2.40	ϕ[C–Cα–N]	0.22 (0.48)
ν[N–H]	5.665	ϕ[Hα–Cα–N]	0.165 (0.80)
ν[Cα–Cβ]	2.90	ϕ[N–Cα–Cβ]	0.22 (0.48)
ν[N==C]	5.26	ϕ[H–Cα–Cβ]	0.345 (0.20)
ν[Cβ–Hβα]	4.195	ϕ[Cα–N==C]	0.65 (0.30)
ν[Cβ–Oα]	3.61	ϕ[Cα–N–H]	0.40 (0.47)
ν[Oα–Cγ]	5.49	ϕ[H–N==C]	0.42 (0.18)
ν[Cγ=Oβ]	10.31	ϕ[Hβα–Cβ–Cα]	0.467 (0.22)
ν[Cγ–Cδ]	3.29	ϕ[Oα–Cβ–Hβα]	0.344 (0.34)
ν[Cδ–Hδα]	4.402	ϕ[Hβα–Cβ–Hββ]	0.442 (0.17)
ν[C==O]	8.85	ϕ[Cα–Cβ–Oα]	0.51 (0.25)
ω[O==C]	0.233	ϕ[Cβ–Oα–Cγ]	0.36 (0.20)
ω[Oβ=Cγ]	0.57	ϕ[Oα–Cγ=Oβ]	0.30 (0.50)
ω[H–N]	0.1568	ϕ[Oα–Cγ–Cδ]	0.51 (0.36)
τ[Cα–N]	0.055	ϕ[Oβ=Cγ–Cδ]	0.57 (0.36)
τ[N==C]	0.035	ϕ[Cγ–Cδ–Hδγ]	0.38 (0.20)
τ[Cα–Cβ]	0.025	ϕ[Hδγ–Cδ–Hδβ]	0.439 (0.215)
τ[Cβ–Oα]	0.030	ϕ[N==C==O]	0.71 (0.70)
τ[Oα–Cγ]	0.090	ϕ[N==C–Cα]	0.21 (0.60)
τ[Cγ–Cδ]	0.035	ϕ[O==C–Cα]	0.395 (0.60)
τ[C–Cα]	0.025		

2.2. Calculation of heat capacity

Dispersion curves can be used to calculate the heat capacity of a polymeric system. For a one-dimensional system the density-of-state function or the frequency distribution function is calculated from the relation

$$g(\nu) = \sum_j (\mathrm{d}\nu_j/\mathrm{d}\delta)^{-1} \Big|_{\nu_j(\delta)=\nu} \tag{3}$$

The sum is over all branches j. Considering a solid as an assembly of harmonic oscillators, the frequency distribution $g(\nu)$ is equivalent to a partition function.

The constant volume heat capacity C_V can be calculated using Debye's relation

$$C_V = \sum_j g(\nu_j) \mathrm{k} N_A (h\nu_j/\mathrm{k}T)^2 \frac{\exp(h\nu_j/\mathrm{k}T)}{[\exp(h\nu_j/\mathrm{k}T) - 1]^2} \tag{4}$$

with

$$\int g(\nu_j)\, \mathrm{d}\nu_j = 1. \tag{5}$$

The constant volume heat capacity C_V given by Eq. (4) is converted into constant pressure heat capacity C_P using the Nernst–Lindemann approximation [18]

$$C_P - C_V = 3RA_0(C_P^2 T/C_V T_m^0) \tag{6}$$

where A_0 is a constant often of universal value $[3.9 \times 10^{-9}$ (K mol) $J^{-1}]$ and T_m^0 is the estimated equilibrium melting temperature.

3. Results and discussion

The unit cell of PALS, as shown in Fig. 1, has 16 atoms giving rise to 48 normal modes and their dispersion. The normal mode frequencies have been calculated for the δ values ranging from 0 to π in steps of 0.05π. The Urey–Bradley force field, which provides a better description of the intra-unit interactions and the interactions between neighboring units, is used for the calculation of normal mode frequencies. Force constants, initially taken from PLS [14] and other molecules having atoms placed in similar environment, have been modified to give the "best fit" to the observed FTIR spectra (shown in Fig. 2). Best fitted force constants are given in Table 1. The assignment of modes is based not only on potential energy distribution (PED) but also on the line intensity and line profile in FTIR. Second derivative spectra have also been very useful in the assignments.

In Figs. 3(a), 4(a) and 5(a) we have plotted the dispersion of modes below 1400 cm^{-1}. All modes with a higher frequency are either nondispersive or show very little dispersion. Four zero frequencies shown in Fig. 5(a) are the four acoustic modes, two of which at $\delta = 0$ correspond to the translations and rotation about the chain axis, the other two

Table 2
Back bone modes

Frequency (cm^{-1})		Assignments %PED at $\delta = 0$	Frequency (cm^{-1})		Assignments %PED at $\delta = \pi$
Calculated	Observed		Calculated	Observed	
3303	3304	ν[N–H](100) (Amide A)	3303	3304	ν[N–H](100)
2962	2962	ν[Cα–H](99)	2962	2962	ν[Cα–H](99)
1640	1641	ν[C==O](71) + ν[N==C](16) (Amide I)	1637	1641	ν[C==O](73) + ν[N==C](14)
1521	1522	ϕ[Cα–N–H](38) + ϕ[H–N–C](33) + ν[N==C](18) (Amide II)	1517	1522	ϕ[Cα–N–H](38) + ϕ[H–N==C](31) + ν[N==C](19)
1229	1225	ν[N==C](35) + ν[C–Cα](13) + ϕ[Cα–N–H](12) + ϕ[N==C==O](7) + ν[Cα–N](6) + H–N==C + ϕ[Hα–Cα–N](5) (Amide III)	1217	1225	ν[N==C](31) + ν[C–Cα](12) + ν[Cα–N](11) + ϕ[Cα–N–H](10) + ϕ[N==C==O](9) + ϕ[O==C–Cα](5)

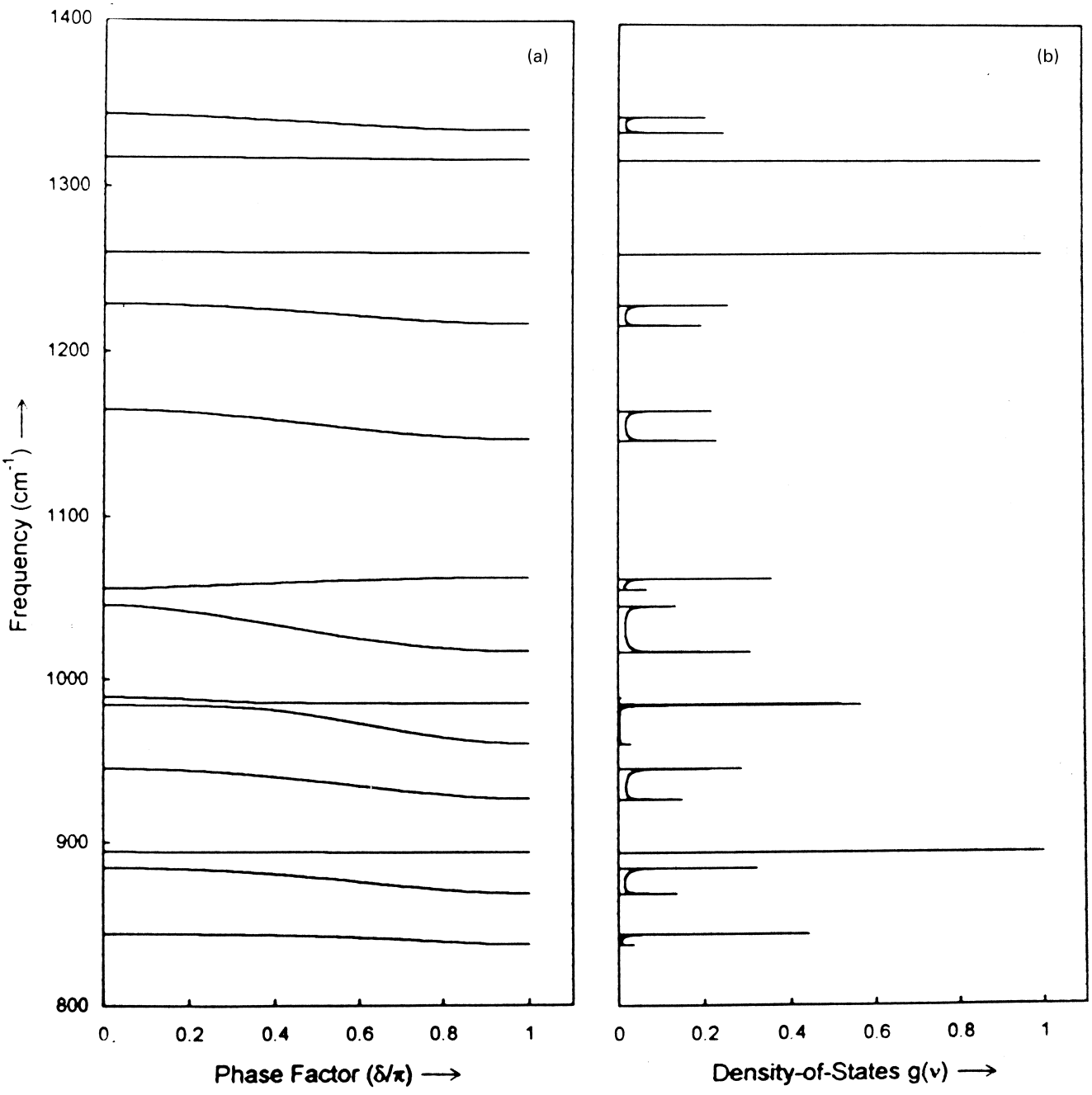

Fig. 3. (a) Dispersion curves of PALS (1400–800 cm^{-1}). (b) Density-of-states $g(\nu)$ (1400–800 cm^{-1}).

at $\delta = \pi$ correspond to translations perpendicular to the chain axis. Pure back bone and pure side chain modes are given in Tables 2 and 4, respectively. The mixed modes which involve a coupling of back bone and side chain modes are given in Table 5. Although the spectra is not available below 600 cm^{-1}, our calculations are expected to be correct for more than one reason. First, they occur in the same range as do these modes in other polymers (Table 3). Second, since the force constants which provide a good matching in the higher frequency region are also involved in the lower frequency region, reasonable values are expected in this region as well.

4. Amide modes

Amide group of polypeptides gives rise to strong characteristic bands usually referred to as amide modes. These amide modes (Amide A, I–VII) are very useful in the determination of the conformation of polymers. Amides I and II solely depend on the conformation of the main chain and are almost unaffected by the side chain conformation. The parallel and perpendicular dichroism of both parallel and antiparallel-β forms have been shown to be opposite to those of the α-helix in the amide I and II regions. The cross-β form is found to have the same dichroism as is

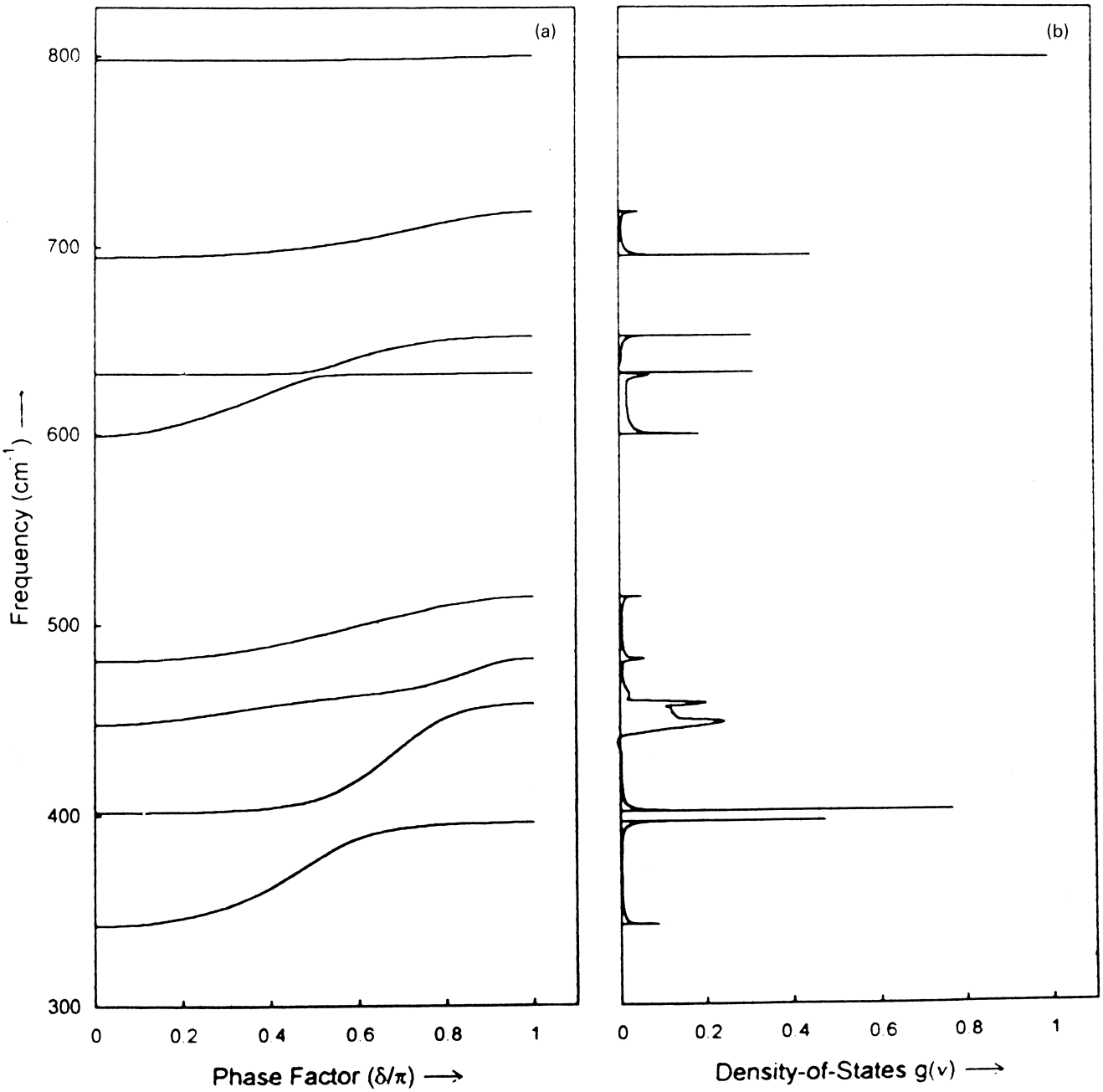

Fig. 4. (a) Dispersion curves of PALS (800–300 cm^{-1}). (b) Density-of-states $g(\nu)$ (800–300 cm^{-1}).

associated with the α-helix (because of the fact that the polypeptide chain is perpendicular to fiber axis) [4], but the amide I and II bands of this β-form appear at the same frequencies as are ascribed to the antiparallel-β form. Other amide modes which although depend on the conformation of side chain but still have a common range for a given main chain conformation. A comparison of amide modes of PALS with other polymers having antiparallel-β sheet conformation is given in Table 3.

Amide A mode which is purely due to the N–H stretch vibration is highly sensitive to the strength of N–H···O=C hydrogen bond. In PALS it is calculated at 3303 cm^{-1} and is assigned to 3304 cm^{-1} whereas in PLS it is calculated at 3318 cm^{-1}. Higher frequency in PLS is attributed to the weaker hydrogen bond strength. Amide I mode having a mixed contribution from stretches of C=O and C=N bonds is calculated at 1640 cm^{-1} and assigned to the peak observed at 1641 cm^{-1} which falls in the same general region (Table 3). The amide II peak is observed at 1522 cm^{-1} and calculated at 1521 cm^{-1}.

Amide III mode does not solely depend on the back bone conformation. Side chain also plays an important role [19]. This mode having contributions from C=N and C–Cα stretches and C=N in-plane bend is calculated at

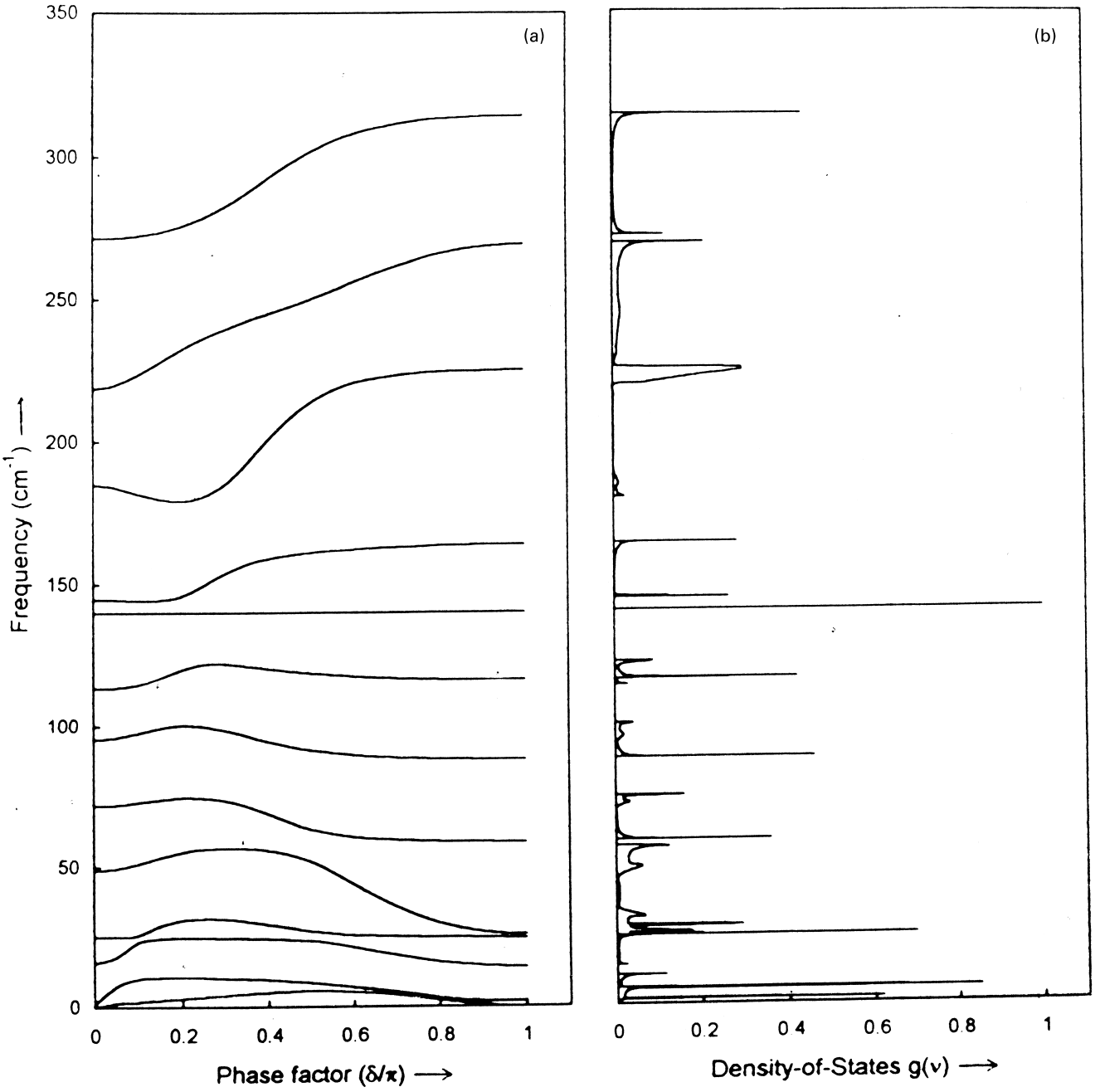

Fig. 5. (a) Dispersion curves of PALS (300–00 cm^{-1}). (b) Density-of-states $g(\nu)$ (300–00 cm^{-1}).

1229 cm^{-1}. This mode corresponds to the observed peak at 1225 cm^{-1}. It is evident from Table 3 that the nature of the side chain does affect this mode. Similarly the amide V, in addition to the main chain and side chain conformation, is also affected by the hydrogen bond strength. The mode calculated at 695 cm^{-1} has major contribution of N–H out-of-plane bend (amide V) and it is assigned to the peak at 696 cm^{-1}. C=O in-plane bending (amide IV) and out-of-plane bending (amide VI) are calculated at 600 and 448 cm^{-1}, respectively.

A comparison of various amide modes of polypeptides having antiparallel-β-sheet confirmation, in particular those which disperse, shows that they have similar profile of dispersion curves although the frequencies both at the zone center and zone boundary are different. This is what one would expect because of the interactions of these modes in a varying degree with the modes belonging to the side chain. Such a comparison between acoustic and low frequency optical dispersion curves exists for polypeptides in similar conformations [20]. As expected the frequencies are again different because of their interactive nature.

Table 3
Comparison of amide modes of β-PALS with other β-sheet polypeptides [All frequencies are in cm^{-1}; PALS: poly(*O*-acetyl, L-serine); PBLC: poly(*S*-benzyl, L-cysteine); PLS: poly(L-serine); PLV: poly(L-valine); PLA: poly(L-alanine).]

Modes	β-PALS		β-PBLC		β-PLS		β-PLV		β-PLA	
	$\delta = 0$	$\delta = \pi$	$\delta = 0$	$\delta = \pi$	$\delta = 0$	$\delta = \pi$	$\delta = 0$	$\delta = \pi$	$\delta = 0$	$\delta = \pi$
Amide A	3303	3303	3291	3291	3318	3318	3290	3290	3283	3283
Amide I	1640	1637	1634	1629	1637	1628	1638	1638	1695	1634
Amide II	1521	1517	1518	1511	1532	1537	1545	1545	1524	1524
Amide III	1229	1217	1261	1222	1249	1270	1228	1228	1224	1241
Amide IV	600	–	617	798	533	773	548	684	594	657
Amide V	695	718	719	668	713	685	715	715	622	705
Amide VI	448	515	525	638	533	647	615	628	594	657

5. Side chain modes

The side chain of PALS consists of a CH_2 group attached with an acetyl group. The modes involving the motion of these atoms are termed as side chain modes and are given in Table 4. The antisymmetric and symmetric CH stretches of CH_2 group calculated at 2896 and 2872 cm^{-1} are assigned to observed peaks at the same value. Symmetric CH stretch of methyl group is calculated at 2961 cm^{-1} (assigned to 2962 cm^{-1}) while the antisymmetric degenerate stretches calculated at 2939 and 2938 cm^{-1} correspond to the observed peak frequency at 2938 cm^{-1}. Being highly localized these modes are observed in the same range in other polypeptides. The observed peak at 1750 cm^{-1} corresponds to the C=O stretch of acetyl group calculated at the same value.

The scissoring vibrations of methyl group are calculated at 1480 and 1468 cm^{-1} which are, respectively, assigned to peaks at 1482 and 1466 cm^{-1} while that of CH_2 group is calculated at 1447 cm^{-1} (assigned to 1446 cm^{-1}). The peak observed at 1379 cm^{-1} corresponds to the symmetric deformation mode of methyl group calculated at 1380 cm^{-1}. The modes calculated at 1260 and 989 cm^{-1} have a major contribution of C–O and C–C stretches of the side chain. These modes are, respectively, assigned to the observed frequencies at 1263 and 993 cm^{-1}.

Table 4
Side chain modes

Frequency (cm^{-1})		Assignments %PED at $\delta = 0$
Calculated	Observed	
2961	2962	ν[Cδ–Hδα](100)
2939	2938	ν[Cδ–Hδα](100)
2938	2938	ν[Cδ–Hδα](100)
2896	2896	ν[Cβ–Hβα](99)
2872	2872	ν[Cβ–Hβα](100)
1750	1750	ν[Cγ=Oβ](76) + ν[Oα–Cγ](11)
1480	1482	ϕ[Hδγ–Cδ–Hδβ](95)
1468	1466	ϕ[Hδγ–Cδ–Hδβ](96)
1447	1446	ϕ[Hβα–Cβ–Hββ](76) + ϕ[Hβα–Cβ–Cα](15)
1380	1379	ϕ[Hδγ–Cδ–Hδβ](37) + ϕ[Cγ–Cδ–Hδγ](34) + ν[Cγ–Cδ](20) + ν[Oα–Cγ](8)
1260	1263	ν[Oα–Cγ](44) + ν[Cγ–Cδ](14) + ϕ[Cγ–Cδ–Hδγ](9) + ϕ[Hδγ–Cδ–Hδβ](8) + ϕ[Oβ=Cγ–Cδ](6)
989	993	ν[Cβ–Oα](33) + ν[Cα–Cβ](22) + ϕ[Cγ–Cδ–Hδγ](6)
894	–	ϕ[Cγ–Cδ–Hδγ](81)
140	–	τ[Cγ–Cδ](93)
113	–	τ[Oα–Cγ](62) + τ[Cα–Cβ](14) + ω[Oβ = Cγ](6)

6. Dispersion curves

Dispersion curves of PALS are shown in Figs. 3(a), 4(a) and 5(a). Since the modes above 1400 cm^{-1} are nondispersive only the modes below this are shown. One of the characteristic features of dispersion curves is the repulsion and exchange of character between various pairs of modes. Such feature is observed for pairs of modes of frequencies 989 and 984 cm^{-1} and 633 and 599 cm^{-1} in the neighborhood of $\delta = 0.5\pi$. It is observed that the modes come closer up to this δ value and diverge thereafter because of repulsion at higher δ values. The regions of high density-of-states where $(\partial\omega/\partial k) \rightarrow 0$ are akin to critical points known as Von Hove singularities in lattice dynamics [21]. They are generally due to internal symmetry points in the energy momentum space. A knowledge of these is important in obtaining several thermodynamic properties such as heat capacity, enthalpy changes, etc. They are more conveniently observable in inelastic incoherent neutron scattering.

The contributions of ν(Cβ–Oα) and ν(Cα–Cβ) in 989 cm^{-1} and that of ϕ(Cγ–Cδ–Hδγ) and ω(Oβ=Cγ) in 984 cm^{-1} mode goes on decreasing till $\delta = 0.5\pi$. The modes come closer upto this δ value where they exchange their PEDs and beyond this the respective contributions in each mode start increasing and the modes diverge from each other. Character exchange and repulsion is also observed for pair of modes of frequency 633 and 599 cm^{-1}. It is observed that the lower frequency mode approaches the higher one upto $\delta = 0.55\pi$. The PEDs of the two modes are exchanged at this δ value. Beyond this the lower frequency mode remains constant at 632 cm^{-1} upto the zone boundary

Table 5
Mix modes

Frequency (cm^{-1})		Assignments %PED at $\delta = 0$	Frequency (cm^{-1})		Assignments %PED at $\delta = \pi$
Calculated	Observed		Calculated	Observed	
1343	1340	ϕ[Hα–Cα–N](36) + ϕ[C–Cα–Hα](17) + ϕ[Hβα–Cβ–Cα](12) + ν[C–Cα](11) + ϕ[Oα–Cβ–Hβα](9)	1334	1340	ϕ[Hα–Cα–N](29) + ϕ[Hβ–Cβ–Cα](17) + ϕ[Oα–Cβ–Hβα](15) + ϕ[C–Cα–Hα](14) + ν[C–Cα](6) + ν[Cβ–Oα](5)
1318	1315	ϕ[Oα–Cβ–Hβα](24) + ϕ[Hβα–Cβ–Cα](20) + ϕ[Hα–Cα–N](16) + ν[Cβ–Oα](10) + ν[Cα–Cβ](9) + ϕ[C–Cα–Hα](5)	1316	1315	ϕ[Hα–Cα–N](24) + ϕ[Oα–Cβ–Hβα](19) + ϕ[Hβα–Cβ–Cα](16) + ϕ[C–Cα–Hα](8) + ν[Cβ–Oα](8) + ν[Cα–Cβ](8)
1165	1167	ϕ[Hβα–Cβ–Cα](45) + ϕ[Oα–Cβ–Hβα](28) + ν[Cα–N](13)	1147	–	ϕ[Hβα–Cβ–Cα](47) + ϕ[Oα–Cβ–Hβα](35) + ν[N==C](7)
1056	1053	ϕ[H–Cα–Cβ](21) + ν[Cα–N](17) + ϕ[Oα–Cβ–Hβα](17) + ν[Cβ–Oα](16) + ν[C–Cα](7) + ϕ[C–Cα–Hα](7)	1063	1053	ν[Cα–Cβ](26) + ϕ[H–Cα–Cβ](26) + ν[Cα–N](10) + ν[Cβ–Oα](9) + ϕ[Oα–Cβ–Hβα](8) + ϕ[Hβα–Cβ–Cα](6)
1045	1047	ν[Cα–Cβ](33) + ν[Cα–N](26) + ϕ[Oα–Cβ–Hβα](11) + ϕ[H–Cα–Cβ](7) + ϕ[Hβα–Cβ–Cα](7)	1017	–	ν[Cβ–Oα](29) + ν[Cα–Cβ](23) + ν[Cα–N](14) + ϕ[Oα–Cβ–Hβα](7) + ϕ[C–Cα–Cβ](5)
984	–	ϕ[Cγ–Cδ–Hδγ](68) + ω[Oβ=Cγ](18)	960	946	ν[Cβ–Oα](30) + ϕ[H–Cα–Cβ](19) + ϕ[C–Cα–Hα](8) + ν[N==C](8) + ϕ[Oα–Cβ–Hβα](7) + ν[Cα–N](6) + ν[C–Cα](6)
945	946	ϕ[H–Cα–Cβ](18) + ν[Cβ–Oα](15) + ν[C–Cα](9) + ϕ[Cα–N–C](9) + ν[C==O](8) + ν[N==C](7)	927	–	ν[Cα–N](27) + ν[Cα–Cβ](16) + ϕ[Cα–N–C](8) + ν[C–Cα](7) + ϕ[H–Cα–Cβ](6) + ϕ[Cα–Cβ–Oα](5)
884	887	ϕ[H–Cα–Cβ](26) + ν[C–Cα](18) + ϕ[C–Cα–Hα](16) + ν[Cα–Cβ](12) + ν[C==O](5)	869	–	ν[C–Cα](28) + ϕ[H–Cα–Cβ](19) + ϕ[C–Cα–Hα](11) + ϕ[Oα–Cβ–Hβα](7) + ν[Cγ–Cδ](5)
844	846	ν[Cγ–Cδ](51) + ν[Oα–Cγ](20) + ν[Cγ=Oβ](9)	837	846	ν[Cγ–Cδ](46) + ν[Oα–Cγ](20) + ν[Cγ=Oβ](8) + ν[C–Cα](8)
798	799	ϕ[Oα–Cβ–Hβα](39) + ϕ[Hβα–Cβ–Cα](38) + ν[Cα–N](6)	800	799	ϕ[Oα–Cβ–Hβα](30) + ϕ[Hβα–Cβ–Cα](27) + ϕ[N==C==O](9) + ν[C–Cα](6) + ϕ[Cα–N==C](5)
695	696	ω[H–N](66) + ω[O==C](11)	718	719	ω[H–N](28) + ν[Cα–N](18) + ϕ[N==C==O](8) + ϕ[Hβα–Cβ–Cα](7)
632	633	ω[Oβ=Cγ](67) + ϕ[Cγ–Cδ–Hδγ](21) + τ[Oα–Cγ](7)	652	661	ω[H–N](50) + ν[Cα–N](8) + ω[O==C](7) + ν[C–Cα](6) + ϕ[O==C–Cα](6)
600	–	ϕ[N==C==O](36) + ϕ[O==C–Cα](20) + ν[C–Cα](9) + ϕ[Cα–Cβ–Oα](6) + ϕ[C–Cα–Cβ](5)	632	633	ω[Oβ=Cγ](67) + ϕ[Cγ–Cδ–Hδγ](20) + τ[Oα–Cγ](7)
481	–	ϕ[Oβ=Cγ–Cδ](35) + ϕ[Oα–Cγ=Oβ](18) + ϕ[Cβ–Oα–Cγ](9) + ω[O==C](6) + ν[Cγ–Cδ](6) + ϕ[C–Cα–Cβ](5)	515	–	ω[O==C](17) + ϕ[C–Cα–N](16) + ϕ[N==C–Cα](14) + ϕ[O==C–Cα](8) + ω[H–N](6) + ϕ[C–Cα–Cβ](5)
448	–	ω[O==C](38) + ω[H–N](14) + ϕ[Oβ=Cγ–Cδ](13) + ϕ[C–Cα–Cβ](11) + ϕ[C–Cα–N](7) + ϕ[Oα–Cγ–Cδ](6)	482	–	ϕ[Oβ=Cγ–Cδ](18) + ϕ[N–C–Cα](16) + ϕ[Oα–Cγ=Oβ](13) + ϕ[N–Cα–Cβ](8) + ϕ[Cβ–Oα–Cγ](8) + ω[O==C](6) + ϕ[O==C–Cα](6)
402	–	ϕ[Oα–Cγ–Cδ](42) + ϕ[Oα–Cγ=Oβ](20) + ϕ[Cα–Cβ–Oα](7) + ϕ[Cβ–Oα–Cγ](6) + ω[O==C](6)	459	–	ϕ[Oβ=Cγ–Cδ](30) + ω[O==C](21) + ϕ[Oα–Cγ–Cδ](11) + ϕ[C–Cα–Cβ](6)
342	–	ϕ[N–Cα–Cβ](21) + ϕ[Cα–Cβ–Oα](17) + ϕ[O==C–Cα](11) + ϕ[Oβ=Cγ–Cδ](7) + ϕ[Cβ–Oα–Cγ](6)	396	–	ϕ[Oα–Cγ–Cδ](37) + ϕ[Oα–Cγ=Oβ](23) + ϕ[Cα–Cβ–Oα](10) + ω[O==C](6)
271	–	ϕ[N–Cα–Cβ](55) + ϕ[Cα–Cβ–Oα](7)	314	–	ϕ[N–Cα–Cβ](21) + ϕ[Cα–Cβ–Oα](16) + ω[O==C](9) + ϕ[Cα–N==C](8) + ϕ[Cβ–Oα–Cγ](6) + ω[H–N](5)
219	–	phi;[C–Cα–Cβ](17) + ϕ[N==C–Cα](12) + ϕ[O==C–Cα](9) + ϕ[C–Cα–N](9) + ν[C–Cα](8) + ϕ[C–Cα–Hα](7) + ϕ[Cα–N–C](6) + ϕ[Cβ–Oα–Cγ](6)	269	–	ϕ[N==C==O](23) + ϕ[O==C–Cα](20) + ϕ[Cα–N==C](13) + ϕ[C–Cα–N](12)
185	–	ϕ[Cα–N–C](34) + ϕ[N==C==O](16) + ϕ[N==C–Cα](12) + ϕ[C–Cα–Cβ](7) + ϕ[H–N==C](6)	225	–	ϕ[N–Cα–Cβ](26) + ϕ[Cα–Cβ–Oα](25) + ϕ[C–Cα–N](10)
145	–	ϕ[C–Cα–N](23) + ϕ[Cα–Cβ–Oα](17) + ω[O==C](12) + ϕ[C–Cα–Cβ](9)	164	–	ϕ[C–Cα–Cβ](30) + τ[Oα–Cγ](12) + ω[O==C](11) + ϕ[N–Cα–Cβ](9) + ϕ[Cβ–Oα–Cγ](6) + ϕ[C–Cα–N](6) + τ[Cα–Cβ](5)
95	–	ϕ[Cβ–Oα–Cγ](39) + τ[Cα–N](11) + ν[Cα–N](7) + τ[Oα–Cγ](6)	88	–	τ[Oα–Cγ](47) + τ[Cβ–Oα](8) + ϕ[Cβ–Oα–Cγ](7) + ϕ[C–Cα–Cβ](7) + ω[Oβ=Cγ](5) + ϕ[N–Cα–Cβ](5)

Table 5 (*continued*)

Frequency (cm^{-1})		Assignments %PED at $\delta = 0$	Frequency (cm^{-1})		Assignments %PED at $\delta = \pi$
Calculated	Observed		Calculated	Observed	
72	–	ϕ[Cβ–Oα–Cγ](24) + ϕ[C–Cα–Cβ](20) + ϕ[Cα–Cβ–Oα](12) + τ[Cβ–Oα](7) + ω[O==C](6) + τ[Oα–Cγ](6)	59	–	τ[Cα–N](43) + τ[C–Cα](18) + ω[O==C](14) + τ[Cβ–Oα](9)
49	–	τ[Cβ–Oα](31) + τ[N==C](24) + τ[C–Cα](10) + ω[O==C](7) + ϕ[C–Cα–N](6)	26	–	τ[Cα–Cβ](21) + τ[Cβ–Oα](21) + ϕ[C–Cα–Cβ](11) + τ[Cα–N](9) + τ[Oα–Cγ](6) + ϕ[Cα–N==C](5)
25	–	τ[Cα–Cβ](50) + τ[Cβ–Oα](31) + τ[Oα–Cγ](11)	24	–	τ[Cα–Cβ](24) + τ[Cβ–Oα](16) + ϕ[C–Cα–Cβ](7) + ϕ[Cα–N==C](6) + τ[Oα–Cγ](5)
16	–	τ[N==C](27) + τ[Cβ–Oα](26) + τ[Cα–Cβ](24) + τ[C–Cα](6)	14	–	τ[Cβ–Oα](40) + τ[Cα–Cβ](35) + ϕ[N–Cα–Cβ](7)
1	–	ϕ[N==C–Cα](26) + ϕ[O==C–Cα](17) + τ[C–Cα](15) + τ[Cα–N](14) + τ[N==C](13) + ϕ[N==C==O](10)	2	–	τ[N==C–Cα](43) + ϕ[O==C–Cα](21) + ϕ[N==C==O](13) + ϕ[N==C–Cα](10)
0	–	ϕ[Oα–Cγ=Oβ](39) + ϕ[Oα–Cγ–Cδ](29) + ϕ[Oβ=Cγ–Cδ](29)	0	–	ϕ[Cγ–Cδ–Hδγ](51) + ϕ[Hδγ–Cδ–Hδβ](46)

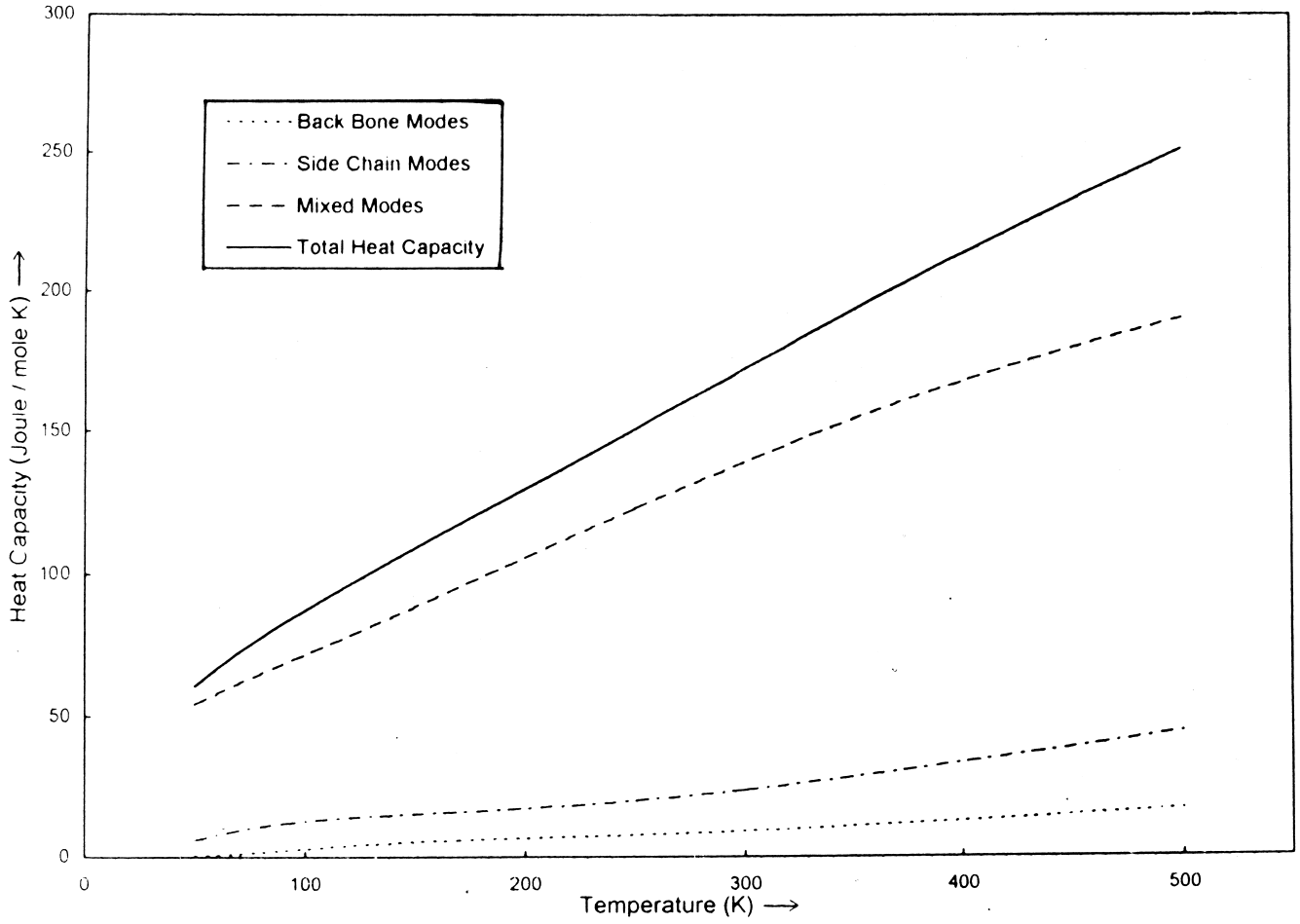

Fig. 6. Variation of heat capacity C_P with temperature.

while the higher frequency mode, which was constant so far, increases to reach 652 cm^{-1} at $\delta = \pi$. This interesting phenomenon of exchange of character may be viewed as the collision of the two phonons approaching each other and exchanging their energy and then moving apart.

The dispersion curves in the lower frequency region (~80–160 cm^{-1}) fan out from the zone center towards the zone boundary, appearing to repel each other. This feature is also observed for the dispersion curves of β-PLS [14], β-poly(L-alanine) [22], polyethylene [23] and polyglycine I [24] which take the planar zig-zag configuration. This common feature may be attributed to the absence of strong intra-chain interactions stabilizing the structure in contrast to strongly hydrogen bonded α-helix.

The four zero frequencies (two at $\delta = 0$ and two at $\delta = \pi$) correspond to the acoustic modes. These represent three translations (one parallel and two perpendicular to chain axis) and one free rotation around the chain. The shape of these is characteristic of the two fold helical chain symmetry and is similar to the other two fold helical polymers like PLS, poly(L-valine) [25], polyethylene, polyglycine, etc. Agreement with the experimental values for frequencies calculated at $\delta = 0$ and $\delta = \pi$ shows that basically the profile of dispersion curves is in general agreement.

7. Frequency distribution function and heat capacity

The state density distribution function, which expresses the way in which energy is distributed among the various branches of the normal modes, is obtained from the dispersion curves for isolated chain of PALS and is shown in Figs. 3(b), 4(b) and 5(b). The peaks in the frequency distribution curves compare well with the observed frequencies. The frequency distribution function can also be used to calculate the thermodynamical properties such as heat capacity, enthalpy changes, etc.

We have calculated the heat capacity of PALS in the temperature range 50–500 K. The modes which are purely skeletal, purely side chain and a mixture of the two are given in Tables 2, 4 and 5, respectively. Their contribution to heat capacity has also been calculated separately and is shown in Fig. 6. It is observed that the maximum contribution comes from the mixed modes which involve the coupling of both back bone and side chain modes. Since no experimental data is available at present only the predictive values are shown here and we hope that experimental measurements will be available soon.

In conclusion it may be mentioned that the contribution from low frequency lattice modes is bound to make an appreciable difference in heat capacity due to its sensitivity to these modes. In order to take into account this contribution the dispersion curves have to be calculated for three-dimensional unit cell which is extremely difficult. It would not only make the problem almost intractable but also involve an enormous number of interactions which are difficult to visualize and quantify.

Acknowledgements

Financial assistance from the Council of Scientific and Industrial Research, New Delhi to N.K.M. and D.K. for the award of Senior Research Fellowship and to V.D.G. for the C.S.I.R. Emeritus Scientist Project and to P.T. from the Department of Science and Technology under the Young Scientist Project is gratefully acknowledged.

References

[1] Misra NK, Kapoor D, Tandon P, Gupta VD. Polymer 1999; in press.
[2] Fasman GD, Blout ER. J Am Chem Soc 1960;82:2262.
[3] Imahori K, Yahara I. Biopolym Symp 1964;(1):421.
[4] Ananthanarayanan VS. J Sci Ind Res 1972;31:593.
[5] Peacok N. Biochim Biophys Acta 1959;32:220.
[6] Geddes AJ, Parker KD, Atkins EDT, Brighton EJ. J Mol Biol 1968;32:343.
[7] Rippon WB, Anderson JM, Walton AG. J Mol Biol 1971;56:507.
[8] Stern A, Gibbson W, Craig LC. Proc Natl Acad Sci USA 1968;61:734.
[9] Ohnishi M, Urry DW. Biochem Biophys Res Commun 1969;36:194.
[10] Misra NK, Kapoor D, Tandon P, Gupta VD. Polymer J 1997;29(11):914.
[11] Kapoor D, Misra NK, Tandon P, Gupta VD. Eur Polym J 1998;34(12):1781.
[12] Kapoor D, Misra NK, Tandon P, Gupta VD, J Polym Sci-Polym Phys 1999; in press.
[13] Misra NK, Kapoor D, Tandon P, Gupta VD. J Macromolecular Sci (Phys) 1999; in press.
[14] Gupta A, Tandon P, Gupta VD, Rastogi S. Polymer 1997;38:2385.
[15] Wilson EB. J Chem Phys 1941;9:76.
[16] Wilson EB, Decius JC, Cross PC. Molecular vibrations: the theory of infrared and Raman vibrational spectra. New York: Dover Publications, 1980.
[17] Higgs PW. Proc R Soc (London) Ser A 1953;220:470.
[18] Wunderlich B, Bu HS. Thermochim Acta 1987;119:225.
[19] Krimm S, Bandekar J. Adv Protein Chem 1986;38:181.
[20] Tandon P, Gupta VD. Proceedings of the Conference on Spectroscopy of Polymers held at the University of Lyon (France), 1996.
[21] Callaway J. Quantum theory of solids. New York: Academic Press, 1974. p. 30.
[22] Krishnan MV, Gupta VD. Indian J Pure Appl Phys 1972;10:210.
[23] Tasumi M, Shimanouchi T. J Mol Spectrosc 1962;9:261.
[24] Gupta VD, Trevino S, Boutin H. J Chem Phys 1968;48:3008.
[25] Burman L, Tandon P, Gupta VD, Srivastava S. Polymer J 1995;27:481.